

Liquefaction of H₂ molecules upon exterior surfaces of carbon nanotube bundles

Sang Soo Han, Jeung Ku Kang, and Hyuck Mo Lee^{a)}

Department of Materials Science and Engineering, KAIST, Daejeon 305-701, Republic of Korea

Adri C. T. van Duin and William A. Goddard III

Materials and Process Simulation Center, California Institute of Technology, California 91125

(Received 9 December 2004; accepted 4 April 2005; published online 12 May 2005)

We have used molecular dynamics simulations to investigate interaction of H₂ molecules on the exterior surfaces of carbon nanotubes (CNTs): single and bundle types. At 80 K and 10 MPa, it is found that charge transfer occurs from a low curvature region to a high curvature region of the deformed CNT bundle, which develops charge polarization only on the deformed structure. The long-range electrostatic interactions of polarized charges on the deformed CNT bundle with hydrogen molecules are observed to induce a high local-ordering of H₂ gas that results in hydrogen liquefaction. Our predicted heat of hydrogen liquefaction on the CNT bundle is 97.6 kcal kg⁻¹. On the other hand, hydrogen liquefaction is not observed in the CNT of a single type. This is because charge polarization is not developed on the single CNT as it is symmetrically deformed under the same pressure. Consequently, the hydrogen storage capacity on the CNT bundle is much higher due to liquefaction than that on the single CNT. Additionally, our results indicate that it would also be possible to liquefy H₂ gas on a more strongly polarized CNT bundle at temperatures higher than 80 K. © 2005 American Institute of Physics. [DOI: 10.1063/1.1929084]

In 1999, Ye *et al.*¹ first reported an experimental finding that bundles of single-walled carbon nanotubes (SWCNTs) could absorb hydrogen in excess of 8 wt % at 100 bar and 80 K. This result satisfies the target of the Department of Energy: namely that hydrogen fuel cell cars require a hydrogen capacity of 6.5 wt % to match the range of a gasoline-powered car. Ye *et al.*¹ suggested that when individual SWCNTs are separated at a pressure higher than 40 bar hydrogen is physisorbed on the exposed surfaces of the SWCNTs. We now report another conclusion. In general, gas molecules form a monolayer surface coverage on solids,² as proved by the well-known Brunauer–Emmett–Teller (BET) theory of adsorption.³ When a surface is completely covered with a monolayer of adsorbate, additional molecules are adsorbed on the first layer of the adsorbate. However, the van der Waals interaction energy of the solid surface with the additional layers is negligible in comparison with the interaction energy of the molecules of the first layer, and it is therefore difficult for additional layers to form. Consequently, this BET theory indicates that the physisorption capacity of hydrogen at a constant temperature has no linear relationship with the gas pressure.⁴ In other words, the hydrogen physisorption capacity initially increases as the gas pressure increases, but then decreases. This phenomenon is called supercritical adsorption.⁴ However, Ye *et al.*¹ experimentally showed that the hydrogen uptake capacity increases almost linearly with the increased hydrogen pressures. In addition, Gao *et al.*⁵ reported that a single CNT with a cap shows a H₂ uptake capacity of less than 2.18 wt % hydrogen at 77 K and 10 MPa. This begs the question of why a high H₂ uptake capacity can only be found in CNT bundles. We therefore examine how hydrogen physisorption behaves on

various surfaces of different CNT structures, particularly under conditions of high pressure and near liquid nitrogen temperature.

To study how hydrogen molecules interact with the surfaces of different CNT structures, we used molecular dynamics (MD) simulations with an isothermal-isobaric canonical ensemble condition. A time step of 0.5×10^{-15} s was chosen to determine the equation of motions of atoms. The interatomic forces between hydrogen and carbon are based on a reactive force field (ReaxFF).⁶ We designed ReaxFF to reproduce the bond distances, energies, and charges of B3LYP (Becke three-parameter plus Lee–Yang–Parr functional) density functional theory (DFT)⁷ calculations for hydrocarbon systems. As shown in several studies,^{6,8–11} the ReaxFF accurately describes the breaking and formation of bonds, as well as atomic charges in polarized systems. To account for the van der Waals interactions between C–C, C–H, and H–H, ReaxFF relies on a distance-corrected Morse potential [Eqs. (1)–(3)], the fitted parameters of which have been reported in detail by Nielson *et al.*¹¹ By including a shielded interaction [Eq. (2)], we avoided excessively high repulsions between bonded atoms (1–2 interactions) and atoms that share a valence angle (1–3 interactions). These interactions are expressed as follows:

$$E_{\text{vdWaaals}} = \text{Tap} \cdot D_{ij} \cdot \left\{ \exp \left[\alpha_{ij} \cdot \left(1 - \frac{f_{13}(r_{ij})}{r_{\text{vdW}}} \right) \right] - 2 \cdot \exp \left[\frac{1}{2} \cdot \alpha_{ij} \cdot \left(1 - \frac{f_{13}(r_{ij})}{r_{\text{vdW}}} \right) \right] \right\}, \quad (1)$$

$$f_{13}(r_{ij}) = \left[r_{ij}^{p_{\text{vdW}1}} + \left(\frac{1}{\gamma_{\text{vdW}}} \right)^{p_{\text{vdW}1}} \right]^{1/p_{\text{vdW}1}}, \quad (2)$$

^{a)} Author to whom all correspondence should be addressed; electronic mail: hmlee@kaist.ac.kr

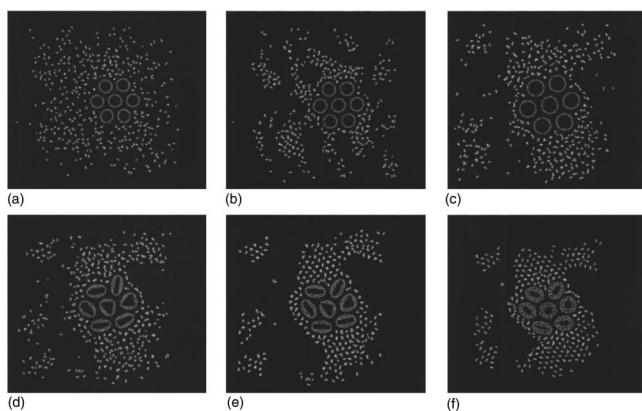


FIG. 1. Interactions of H_2 molecules on the (5,5) SWCNT bundle surfaces at 80 K and 10 MPa. They are obtained from MD simulations employing the ReaxFF, where (a)–(f) indicate snapshots at 0, 2.5, 25, 27.5, 30, and 50 ps, respectively. The grey color represents carbon atoms while the white one represents hydrogen.

$$\text{Tap} = \frac{20}{R_{\text{cut}}^7} \cdot r_{ij}^7 - \frac{70}{R_{\text{cut}}^6} \cdot r_{ij}^6 + \frac{84}{R_{\text{cut}}^5} \cdot r_{ij}^5 - \frac{35}{R_{\text{cut}}^4} \cdot r_{ij}^4 + 1. \quad (3)$$

The term Tap in Eq. (3) is used to avoid energy discontinuity out of the nonbonded cutoff radius ($R_{\text{cut}} = 10.0 \text{ \AA}$) of the ReaxFF. The terms in this polynomial were chosen to ensure that the first, second, and third derivatives of the nonbonded interactions to the distance were all continuous and went to zero at the cutoff boundary. This force field can therefore appropriately describe the weak van der Waals interaction, even for a long range of up to 10.0 \AA . In using ReaxFF, we found that the physisorption energy of a H_2 molecule on the exterior wall of a (5,5) SWCNT is -1.23 kcal/mol , which falls in the physisorption energy range (-0.2 to -2.0 kcal/mol) on a graphene, calculated with several methods: the second-order M\"oller-Plesset perturbation theory; local density approximation, Slater exchange plus Vosko–Wilk–Nusair correlation; generalized gradient approximation, Becke exchange plus Lee–Yang–Parr correlation); and hybrid DFT (B3LYP) by Okamoto and Miyamoto.¹² As a result, we can rely on ReaxFF to adequately explain the van der Waals interaction of hydrogen molecules on the CNT wall.

To model the CNT bundle, we used seven (5,5) SWCNTs with a gap of 3.4 \AA between two of the SWCNT walls. The gap is similar to the graphite interplanar distance. In addition, to simulate how the H_2 molecules interact with the CNT bundle, we used 840 carbon atoms and 400 hydrogen molecules. On the other hand, we used a (10,10) SWCNT to model a single SWCNT and a (5,5) at (10,10) multiwalled CNT (MWCNT) to model a single MWCNT. The box size for all the MD simulations was $70 \text{ \AA} \times 70 \text{ \AA} \times 4.66 \text{ \AA}$, and the periodic boundary condition was applied. Because our simulation focused on the way H_2 molecules interact with the exterior surfaces of the nanotubes, we did not explore how hydrogen molecules interact with carbon atoms inside the tube. During the MD simulations, we applied the pressure hydrostatically.

Figure 1 shows the MD simulation results on the behavior of hydrogen gas with a CNT bundle at 80 K and 10 MPa. The H_2 molecules physically adsorb on the surfaces of the bundle at 2.5 ps with a monolayer coverage and then come together with each other. The gathering degree of the hydro-

gen increases as the simulation time increases. At 27.5 ps, the SWCNT bundle is distorted under a high pressure of 10 MPa. After 30 ps, a high local-ordering of hydrogen is observed near the surfaces, indicating that the hydrogen liquefies. Furthermore, although not shown here, the total energy decreases abruptly between 27.5 and 30 ps. The enthalpy is a sum of the total internal energy for all the atoms and the external energy of $P\Delta V$, where P is the applied pressure and ΔV is the volume change. Because the $P\Delta V$ term in our simulation is negligible compared to the internal energy, the enthalpy can be approximated to the internal energy. Consequently, the predicted energy difference of 97.6 kcal/kg between 27.5 and 30 ps can be considered as the latent heat of vaporization, which is consistent with the experimental value of 108.0 kcal/kg .¹³ Ye *et al.*¹ suggested that the CNT bundle would expand under a high pressure and that the individual SWCNTs should be separated. However, in our MD simulation, the bundle does not appear to expand but rather to contract, and no H_2 molecule was adsorbed among the SWCNT bundle. As shown by Lawrence and Xu,¹⁴ the resistance measurement from a purified SWCNT bundle at room temperature reveals that the bundle was compressed under a high external pressure. This leads to a slight increase in conductivity when the pressure is increased. During the simulation, we also observed no chemisorption of hydrogen gas on the CNT surface. According to our DFT calculation,¹⁵ the chemisorption reaction is endothermic by 18.4 kcal/mol , and its high transition state barrier of 78.3 kcal/mol indicates that there is a kinetic difficulty that may prevent chemisorption from taking place. From these results, we conclude that the increased H_2 uptake capacity on the CNT bundle at 80 K and 10 MPa can be attributed to the liquefaction of the H_2 gas. Our results also account for other phenomena reported by Ye *et al.*¹ For instance, the kink that occurs at around 4 MPa and the steep slope of the hydrogen adsorption isotherm at pressures between 4 and 10 MPa. From the MD simulations, we observe that the liquefaction of H_2 molecules on the CNT bundle occurs at pressures higher than 2 MPa at 80 K. At pressures lower than 2 MPa, the H_2 molecules are physically adsorbed on the CNT bundle with a monolayer coverage. We also investigated the hydrogen-adsorption behavior on the CNT bundle at 300 K and 10 MPa. After 50 ps, the CNT bundle and hydrogen molecules resemble their initial geometries. The H_2 molecules fail to penetrate the interstices of the tubes but wander on the exterior surfaces of the tubes. This phenomenon supports the experimental observation of Lawrence and Xu¹⁴ that the hydrogen adsorption capacity is very low at 300 K and 10 MPa. They showed that only 0.6 wt % hydrogen molecules adsorb on the CNT bundle at 294 K and 10 MPa.

We also examined whether the liquefaction of H_2 molecules can occur on a single CNT. Figure 2 represents MD simulations of H_2 molecules interacting with the surfaces of a single SWCNT and a MWCNT at 80 K and 10 MPa. After 50 ps, no liquefaction of H_2 molecules is found. In these cases, the enthalpy change that signals a phase transition from gas to liquid is not observed. Furthermore, Figs. 2(c) and 2(f) show that when H_2 is about 2.9 \AA from the CNT surface in the early simulation period the H_2 molecules adsorb on the SWCNT and MWCNT surfaces with a monolayer coverage. As with the bundle, the CNT in these cases is distorted under a high pressure. Moreover, because H_2 molecules adsorb on the single CNT surface at 80 K irrespective

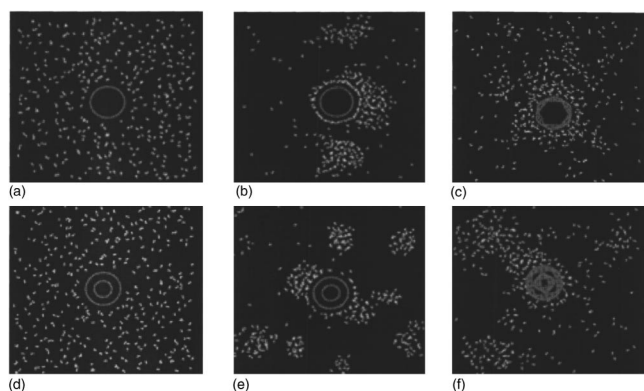


FIG. 2. Interactions of H_2 molecules on the single (10,10) SWCNT and the single (5,5) at (10,10) MWCNT at 80 K and 10 MPa. They are obtained from MD simulations employing the ReaxFF, where (a)–(c) are for the SWCNT and (d)–(f) for the MWCNT. (a) and (d) are taken at 0 ps, (b) and (e) at 10 ps, and (c) and (f) at 50 ps. The grey and white colors represent carbon atoms and hydrogen atoms, respectively.

of pressures, H_2 adsorption capacities on the single SWCNT and the single MWCNT are computed to be lower than that of the CNT bundle, which was proven by the previous work.⁵

Remarkably, the liquefaction of H_2 molecules occurs only with a CNT bundle, and not with a single SWCNT or a single MWCNT. Of all the MD simulation data on the interactions of H_2 molecules with single and bundle types, the only noticeable difference occurs on the structures of the CNTs distorted under a high pressure. The SWCNT bundle deforms into oval shapes under high pressure, as shown in Fig. 1(f), while the shapes of the single SWCNT and MWCNT structures are almost symmetrical, as shown in Figs. 2(c) and 2(f). A recent DFT study¹⁶ showed that if the SWCNT deforms into an oval shape the electron charges transfer from a low-curvature region to a high-curvature region. This charge transfer on the SWCNT bundle develops polarized charges on the CNT structures. Therefore, when the CNT deforms into the oval shape, the electrostatic interaction between the polarized charges on the deformed nanotubes and the induced quadruple charge moments on the hydrogen molecules could result in a high ordering of hydrogen molecules. In a single SWCNT and MWCNT, the phenomenon of the charge transfer is not observed due to the symmetrically deformed shapes. Thus, the local ordering of hydrogen is not observed. This finding has also been supported by a study of Simonyan *et al.*,¹⁷ who used a grand canonical Monte Carlo simulation to investigate the adsorption of hydrogen gas on the charged CNT. Their study showed that H_2 molecules can be adsorbed on charged CNT surfaces due to the interactions between the monopole charges on the CNT and the induced charges on the H_2 . On the other hand, the

long-range electrostatic interaction between the dipole charges on deformed SWCNTs and the induced quadruple charge moments on the H_2 is considered to be responsible for aligning the adsorbed hydrogen along the locally ordered CNT structures. This process eventually makes the hydrogen molecules condense into a liquid state.

In summary, we observed an interesting phenomenon in which hydrogen gas molecules transformed into a liquid phase at around 80 K and 10 MPa on the surfaces of a CNT bundle due to the long-range electrostatic interaction with the deformed, oval-shaped CNT. Liquid hydrogen has good potential as a hydrogen fuel for vehicular transport because it has a high mass density (70.8 kg m^{-3}) and is relatively safe. Despite these advantages, the liquefaction of hydrogen is expensive and requires an intensive cryogenic process for cooling due to the low condensation temperature (21.2 K at 1 bar).¹³ On the other hand, the high liquefaction temperature of hydrogen at around 80 K on a moderately polarized CNT bundle implies that H_2 gas could be liquefied on a more strongly polarized CNT bundle at the temperatures higher than 80 K.

This research was supported by a grant (Code No. 04K1501-02210) from “Center for Nanostructured Materials Technology” under “21st Century Frontier R&D Programs” of the Ministry of Science and Technology, Korea.

¹Y. Ye, C. C. Ahn, C. Witham, B. Fultz, J. Liu J, A. G. Rinzler, D. Colbert, K. A. Smith, and R. E. Smalley, *Appl. Phys. Lett.* **74**, 2307 (1999).

²B. A. Beebe, J. Biscoe, W. R. Smith, and C. B. Wendell, *J. Am. Chem. Soc.* **69**, 95 (1947).

³S. Brunauer, P. H. Emmett, and E. Teller, *J. Am. Chem. Soc.* **60**, 309 (1938).

⁴Y. Zhou, K. Feng, Y. Sun, and L. Zhou, *Chem. Phys. Lett.* **380**, 526 (2003).

⁵H. Gao, X. B. Wu, J. T. Li, G. T. Wu, J. Y. Lin, K. Wu, and D. S. Xu, *Appl. Phys. Lett.* **83**, 3389 (2003).

⁶A. C. T. van Duin, S. Dasgupta, F. Lorant, and W. A. Goddard III, *J. Phys. Chem. A* **105**, 9396 (2001).

⁷A. D. Becke, *J. Chem. Phys.* **98**, 5648 (1993).

⁸A. C. T. van Duin, A. Strachan, S. Stewman, Q. Zhang, X. Xu, and W. A. Goddard III, *J. Phys. Chem. A* **107**, 3803 (2003).

⁹A. Strachan, A. C. T. van Duin, D. Chakraborty, S. Dasgupta, and W. A. Goddard III, *Phys. Rev. Lett.* **91**, 098301 (2003).

¹⁰Q. Zhang, T. Çağın, A. C. T. van Duin, W. A. Goddard III, Y. Qi, and L. G. Hector, *Phys. Rev. B* **69**, 045423 (2004).

¹¹K. D. Nielson, A. C. T. van Duin, J. Oxgaard, W.-Q. Deng, and W. A. Goddard III, *J. Phys. Chem. A* **109**, 493 (2005).

¹²Y. Okamoto and Y. Miyamoto, *J. Phys. Chem. B* **105**, 3470 (2001).

¹³L. Zhou, *Renew. Sust. Energ. Rev.* **9**, 35 (2005).

¹⁴J. Lawrence and G. Xu, *Appl. Phys. Lett.* **84**, 918 (2004).

¹⁵S. S. Han and H. M. Lee, *Carbon* **42**, 2169 (2004).

¹⁶S. B. Fagan, R. Mota, A. J. R. de Silva, and A. Fazio, *Nano Lett.* **4**, 975 (2004).

¹⁷V. V. Simonyan, P. Diep, and J. K. Johnson, *J. Chem. Phys.* **111**, 9778 (1999).